LAI Assimilation Schedules to Constrain Uncertain Cultivars and Soils in CERES-Maize

Luke Monhollon[1,2], Alex C. Ruane[1], William D. Batchelor[3]
[1]NASA Goddard Institute for Space Studies, New York, NY, USA
[2]Autonomic Integra, Bethesda, MD, USA
[3]Auburn University, Auburn, AL, USA

May 25th, 2026

Revision for Computers and Electronics in Agriculture

Corresponding Author: Alex Ruane (alexander.c.ruane@nasa.gov)

Keywords: DSSAT; LAI; remote sensing; CERES-Maize; data assimilation; cultivars; soils; corn; Iowa; AgMIP; MODIS; Phenology

Highlights

- Demonstrated low computational cost remote sensing assimilation for corn model
- Satellite LAI was integrated into CERES-Maize model by using the DSSAT Pest Module
- Observational constraint benefit was sensitive to assimilation timing and schedule
- LAI reduced biases from incorrect cultivars, particularly for early season growth
- Findings further remote sensing assimilation and support broad domain applications

Abstract

In anticipation of large-domain crop model applications where precise local configuration and calibration is not possible, we describe benefits and potential drawbacks of employing a crop pest module to achieve leaf area index (LAI) assimilation into a high performing CERES-Maize crop model configuration at a field experiment site in Perry, Iowa. Simulation experiments explore the use of MODIS satellite-derived LAI to constrain and adjust LAI to counter imprecise cultivar and soil configurations often occurring in the absence of high-quality local information. Simulations using single-day, window, and continuous LAI replacement across 5 cultivars and 2 soil calibration approaches for nine corn rotation years from 2004-2020 led to different yield outcomes and reverberations throughout the field environment. Evaluating variance and mean bias, results indicate minimal interventions in early vegetative and grain-filling stages were more beneficial than use of continuous LAI adjustments, as they minimized disruptions to the internal resource balances governing plant stresses and grain production. LAI adjustment was particularly helpful in constraining growth related to uncertain thermal unit requirements and leaf tip appearance rates (P1 and PHINT cultivar parameters, respectively). Findings underscore the need to assimilate additional state variables to ensure internal biophysical coherence. This approach shows promise for applications spanning wider domains with prediction time pressure where detailed configuration, more complex assimilation methods, or recalibration of crop model parameters may not be practical.

1 Introduction

A core concept behind data assimilation methods is that model simulations accumulate bias with each time step due to imperfections in input data or the model representation of processes. To address this issue, within-simulation updates using observations as additional inputs can serve as a constraint on model conditions keeping the simulation more in line with true conditions. With more accurate (or representative) data reflected in the model, subsequent calculations will produce higher quality predictive results. Enhancing crop model capabilities would benefit decision support applications by agricultural sector stakeholders ranging from farmers to agricultural suppliers and commodity traders. Several studies have demonstrated that a remote sensing constraint improves model performance on a field level or in small-scale domains (Ines et al 2013, Bandaru et al 2022); however, remote sensing-based data assimilation is not broadly utilized within agricultural modeling community networks such as the Agricultural Model Intercomparison and Improvement Project (AgMIP; Rosenzweig et al., 2013; Ruane et al., 2017). In this study, we propose a method to advance data assimilation in process-based crop models, which simulate plant growth in response to genetics, environment (soils and weather), and farm management.

Recent years have seen increasing calls for the development of advanced agricultural modeling systems incorporating crop models, data assimilation, and machine learning, sometimes linked to ‘digital twins’ (Rosenzweig et al. 2023; Pylianidis et al., 2021; Purcell and Neubauer, 2023). This ambition is also central to the goals of the AgMIP community, including as a focus for next-generation crop model development (Jones et al., 2017) and the creation of new machine learning tools (Sweet et al., 2024).

The development of decision support systems utilizing process-based crop models with remote sensing data assimilation has been hindered by two major barriers which are increasingly surmountable. First, previous attempts were limited by computational resources given the diversity of farming systems that must be represented at small scales. The time necessary to execute potentially thousands of iterations is beyond a reasonable lag time to support decision makers. Execution times are further increased for methods interrupting and restarting streamlined models to perform in-season data assimilation. Recent advances in the power and speed of high-performance computational systems and model engineering facilitate parallel processing of large grids at high spatial resolutions, opening up tremendous cost-efficient opportunities. Second, operational systems previously lacked sufficient data to configure and drive large-domain crop models. Today ground surveys, satellite, drone remote sensing, and data collection technologies mounted on field equipment have created a new, data rich environment (Jin et al., 2018). As these barriers fall, new challenges emerge in developing capabilities to assimilate new datasets into high-performance model configurations. Specifically, a need exists for (i) new connection points where assimilated data can constrain model simulations, and (ii) new biophysical process insight allowing models to most effectively represent information conveyed in observational data constraints (Jin et al. 2018, Basso et al 2013). New modeling and assimilation capabilities will likely identify additional data requirements and observational gaps.

The current state of crop model data assimilation reflects these limitations in data assimilation entry points. Previous studies largely targeted an improved calibration with no within-season (e.g., day by day) updates once the simulation begins (Fang et al., 2011; Martre et al 2015; Durand et al 2018; Jin et al. 2018). Adjustments are often targeted across multiple state variables in an effort to maintain consistency and reasonable relationships between nutrient pools. For example, Richetti et al. (2019) compared observations of crop growth stages with first-pass simulations to optimize genotype cultivar parameters prior to a subsequent free-running simulation. This approach places potentially undo pressure on a small set of calibration parameters to correct biases, which can be problematic given the sources of bias are rarely known and isolated. Some studies have shown within-season assimilation of remote sensing data to update model state variables can lead to improvements in model performance, but with high computational expense and requiring novel model components that are not widely available (Ines et al., 2013; Bandaru et al., 2022). Of note, Ines et al (2013) integrated leaf area index (LAI) and soil moisture with notable improvement when modeling maize in Story County, IA, but required interrupting the crop model, performing an Ensemble Kalman filter assimilation method and reinitializing the model at each assimilation point. Adjustments were made across multiple state variables, although the effect on computational speed (a major concern for broader domain studies) was not discussed. A key gap is present addressing model response to data assimilation without modifying all nutrient pools.

This study quantifies errors induced during the assimilation of satellite-estimated LAI into the CERES-Maize model utilizing a simple updating method that affects LAI but does not alter complementary state variables. This approach was examined not as a long-term technical solution, but as a necessary and illustrative step in the development of a new generation of crop model data assimilation. Special consideration was given toward the effect of assimilation on yield, which was the focus of this application. The objectives of this study were to: (1) explore impacts of LAI assimilation through the pest coupling module of CERES-Maize with limited state variable consistency, (2) evaluate how LAI assimilation compensates for poor genetic or soil characterization, and (3) determine which assimilation schedule is the best when compared to a calibrated model.

2 Methods

From prior work, a baseline of expected field performance was generated from a well calibrated version of the Decision Support System for Agrotechnology Transfer (DSSAT; Hoogenboom et al., 2019) model from even years between 1994-2002. Next, we described modifications to the pest/disease coupling points within the CERES-Maize model distributed with the DSSAT crop modeling system enabling measured LAI values to be integrated into simulations of maize production near Perry, Iowa, USA, between 2004 and 2020. Combining the baseline model and with the LAI assimilation method, we explored three LAI assimilation updating strategies: single-day, continuous, and window. Yield predictions were compared to the baseline model.

2.1 Crop Model Calibration

The field used in this study was referred to in various publications as the McGarvey field in Perry, IA (Thorp et al., 2005; Thorp et al., 2006; Batchelor et al., 2002). Here we provide an overview of the field study and prior crop model calibration, with further specifics of the calibration provided in the above-referenced studies. This 20-ha field was divided into 100 grids approximately 0.2 ha in size to represent variations in field characteristics and management in the region. Plant populations were measured in each grid each year, but populations were relatively uniform across grids and years. Management information including planting date, row spacing, nitrogen (N) fertilizer rate, and hybrid were available for each plot. Weather data were collected at the site each year. Yield data was collected by a yield monitor for 1994, 1996, 1998, 2000 and 2002 and averaged for each grid. Calibration data was used from prior studies. No new data was collected or utilized in this study.

In previous work, the CERES-Maize v3.5 model was used to calibrate two soil parameters to minimize error between simulated and observed yield in the 100 unique 0.2 ha grids within a 20 ha field in Perry, IA (Fig. 1). Five seasons of maize yield data were available for 1994, 1996, 1998, 2000 and 2002. (Thorp et al., 2006; Thorp et al., 2007)). The field was divided into 100 grid cells approximately 0.2 ha in size (Figure 1). The CERES-Maize v3.5 model was linked to an optimizer that used a simulated annealing algorithm to optimize two soil parameters related to the effects of tile drainage on crop growth and yield. Cultivar coefficients for the maize hybrid were available. Their results yielded an overall RMSE of 490 kg ha^{-1} and an r^2 of 0.89 between simulated and observed yields over 100 grids and 5 seasons of data.

Thorp et al. (2007) calibrated this field using CERES-Maize v3.5. For this work, we recalibrated soil inputs for each of the 100 grids using CERES-Maize v4.8. Recalibration was necessary because CERES-Maize v3.5 had a modified root growth model that was substantially different compared to the current root growth model in v4.8. These differences affect root depth and distribution dynamics and water stress patterns. The five soil parameters that were calibrated include: 1) RHRF – root shape factor; 2) PASW – percent available soil water (cm^3 cm^{-3}); 3) ETDS – effective tile drain spacing (m); 4) KSAT – saturated hydraulic conductivity of the bottom soil layer (cm d^{-1}); and 5) SLNF – soil nitrogen mineralization rate factor (0-1.0). Parameters ETDS and KSAT affect the efficiency of the subsurface tile drain to control the water table depth in these impermeable soils. The RHRF parameter changes the distribution of roots (root length volume) in soil layers below 60 cm, which affects water uptake in deeper soil layers and ultimately, water stress. The parameter PASW was introduced to make slight adjustments to the lower limit of water holding capacity across all soil layers in a grid, resulting in slightly more or less water holding capacity in the soil. The SLPF parameter is a scalar (0-1.0) that modifies daily photosynthesis rate due to unknown fertility issues or pH problems.

Following the methods outlined in Thorp et al. (2007), crop model input files were established for each grid and season. The crop model was linked to the Geospatial Simulator optimization package (Thorp et al., 2013) that is a plug-in to the QGIS software package (a free and open-source geographic information system suite). Thorp et al. modified the model such that the five parameters could be passed from the optimizer to the crop model during the parameter optimization process. Uncalibrated soil data was extracted from SSURGO to produce field maps. The field map with grid boundaries were imported into QGIS and an attribute table was constructed for grids. The attribute table contained columns for simulated and observed yield for each year, as well as a column for each parameter to be optimized. Rows in the attribute table represented individual grids. The Geospatial Simulation plug-in utilizes the simulated annealing algorithm for parameter optimization. Parameters required to run the optimization were taken from Thorp et al. (2007), who also used the simulated annealing method to calibrate this same field. Different parameter combinations were tested to determine the best combination of parameters that minimized the overall RMSE and R^2 between simulated and observed yields for each grid over 5 seasons.

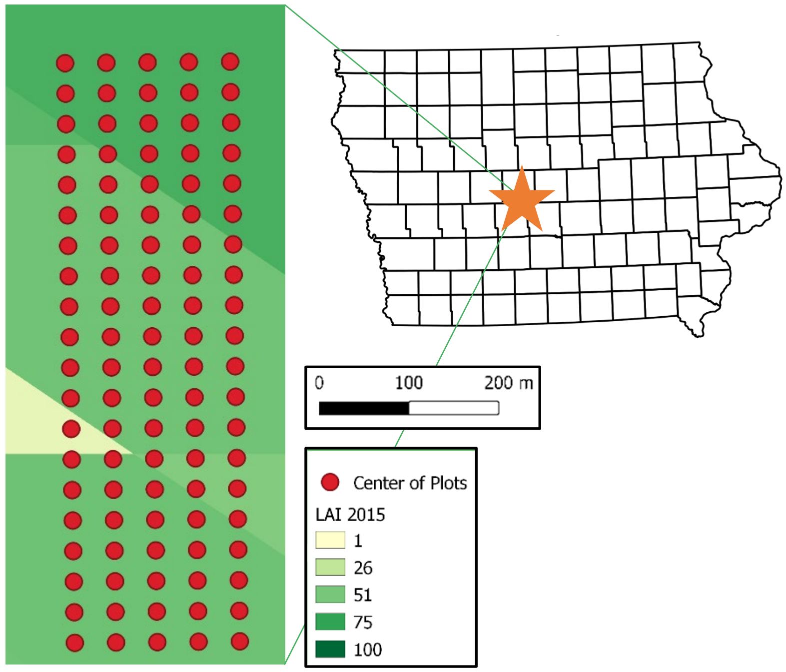

Figure 1*. Location and arrangement of field plot centroids near Perry, Iowa (see inset map) relative to MODIS gridded Leaf Area Index (LAI) for 2015.*

One challenge in using crop models to estimate spatial yields across the landscape is the uncertainty in model inputs including variety and soil properties. The goal of this research was to determine if incorporating remotely sensed LAI as an adjustment to the model can overcome uncertainty in cultivars and soil properties. The results of the baseline model are shown in Figure 2. The baseline model gave good results, with an RMSE of 445.9 kg/ha and R^2 of 0.87 between simulated vs observed yield data over five years and 100 grids.

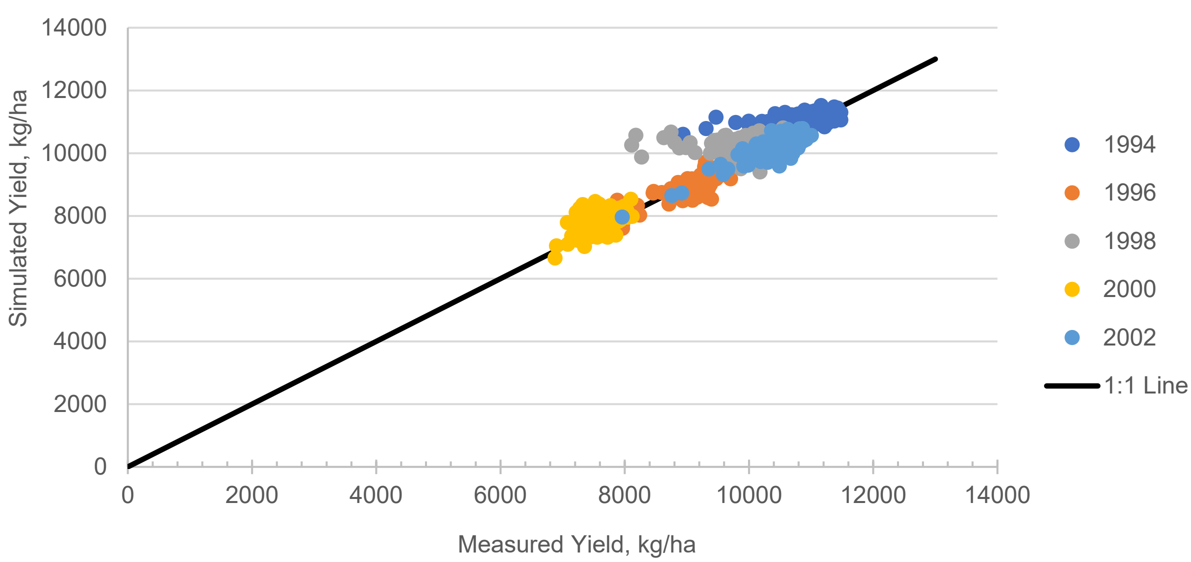

Figure 2. *Mean correspondence between calibration and generic options without LAI assimilation for calibration period at McGarvey Field near Perry, Iowa, differentiated by experimental year.*

Based on these excellent results, we used the baseline model to test different strategies of incorporating remote sensed LAI as an adjustment to the model for different assumptions about genetics and soil properties for the 100 grids in this field. The calibrated model was run for even years (the maize rotation) from 2004-2020 using different combinations of LAI adjustment strategies, and different cultivars and neighboring soil types (assuming no error in boundaries of digital soil maps) to determine how errors in cultivar selection and gridded soil maps may affect simulated yield, and to determine if LAI adjustments could overcome these discrepancies between in-field and simulated results. Inputs for the years 2004-2020 were assumed based on management practices in 2000 and 2002. The maize cultivar was assumed to be PC0004 (distributed with DSSAT v4.8) and the planting date was assumed to be Julian day 117 for each year. Plant populations were maintained from the prior studies, averaging 7.4 pl/m^2, while N application rate was assumed to be 40 kg ha^{-1} applied in the fall followed by 160 kg ha^{-1} applied just before planting. Harvest date was set to maturity. Five soil types were used across the plots: Canisteo silty clay loam, Clarion loam, Nicollet loam, harps loam, and Okoboji silty clay loam. Weather was downloaded from the National Aeronautics and Space Administration (NASA) Langley Research Center Prediction of Worldwide Energy Resource (POWER) project (White et al., 2008).

2.1.1 Incorporating Remote Sensed LAI Adjustments in CERES-Maize

Batchelor et al. (1993) incorporated pest damage routines into the DSSAT family of crop growth models. They defined a series of pest coupling points for leaf, stem, pod, seed, and root damage. Users enter pest damage in a time series pest progress file (File T), and the pest damage is applied on the user defined date entered in File T. The CERES-Maize model distributed in DSSAT v4.8 was modified to adjust LAI, leaf weight, and leaf N content on a user defined (target) date. The new pest input was defined as a Target LAI value derived from remote sensed data that can be applied on one or more user defined dates. Details of the model modification are shown in Appendix 1. Essentially, the Pest module allows a user to impose decreases in LAI as if they were the result of pest damage. This module also allows increases in LAI as if they were the result of a 'negative pest', which is not feasible but an effective mirror image to pest damage allowing DSSAT to expand plant leaf area. The LAI reported by DSSAT at the end of each day is the result of the prior LAI condition, any assimilated LAI information, and any change in LAI resulting from that day's biophysical processes. In application, this results in DSSAT reporting an LAI close to the assimilated LAI but not the exact value.

2.2 Leaf Area Index

2.2.1 LAI Data Sources

We elected to use the combined AQUA-TERRA MODIS 4-day product downloaded for even years from 2004 to 2024 for the McGarvey field from NASA Earthdata (Myneni et al., 2021). This dataset is compatible with NASA HEGTool for simple preprocessing. This dataset features a 500m grid cell size and a 4-day temporal resolution. This is finer than comparable datasets, allowing multiple grid cells to overlap the field and allowing greater granularity and number of assimilation events during the growing season.

2.2.2 Remote Sensed LAI Processing for Crop Model Adjustments

Data assimilation with the LAI product is complicated by the presence of diverse fields, roads, trees, buildings, and non-agricultural land uses that may also be present in any given MODIS grid cell (see Figure 1 for a snapshot of the selected LAI product overlaid with the centers of the field plots). To reduce the effect of minor biases that can cause large spikes or drops in LAI, we investigated three methods to smooth the MODIS 4-day product across (1) time, (2) space, and (3) a combination of time and space. Temporal averaging used a rolling mean of the previous, present, and future measurements in each grid cell (3 measurements in an 9-day period). Spatial averaging used an unweighted average of the nine neighboring grid cells centered on the selected location (effectively increasing the horizontal resolution to 1km^2). Combining both approaches provides stronger spatiotemporal smoothing. We elected to utilize the time averaged MODIS product (#2) in the simulations given the spatial averaging showed substantial volatility and the combined temporal and spatial method showed a lower peak than raw values (influenced downward by neighboring pixels) and washed out some of the spatial detail desired for future field applications.

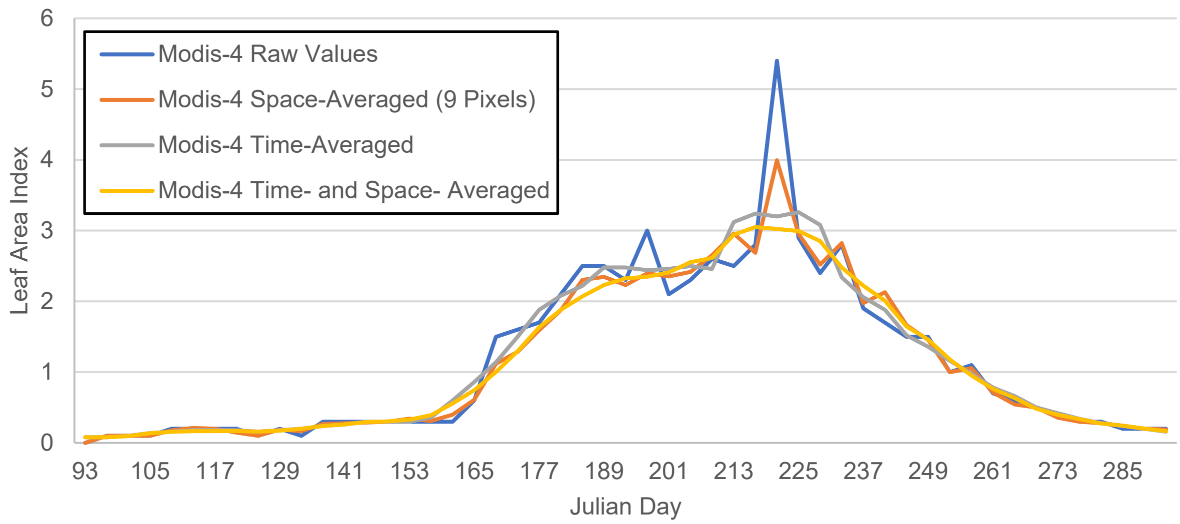

***Figure 3**. The effects of spatial and temporal smoothing on MODIS 4-day LAI observations for 2003.*

2.3 Simulation Experimental Design

We simulated maize seasons from 2004-2020 using the calibrated genetic coefficients and soils for each grid in the field. We used the baseline model as our basis for comparison given accurate estimations of maize yield and excellent spatial performance during the 1994-2002 calibration period. To test the uncertainty of using LAI updating from remote sensing to compensate for uncertainty in soil properties and cultivars, we developed 150 simulation scenarios covering combinations of 2 soil calibrations from the field, 5 cultivars, and 15 LAI assimilation strategies, as described in the section below. Each were tested across 100 grid locations in the study field to explore different levels of field information availability and the incorporation of satellite observations against the baseline (unmodified) model.

To determine a modified model's performance, two statistical tests were applied. Coefficients of determination (R^2) were calculated to evaluate the ability of a model to capture yield variation. Z-scores were calculated to evaluate the statistical significance of mean bias. Z-scores represent how different a sample model's mean is from the perfect model's mean as measured against the perfect model's standard deviation. Z-scores were converted to p-values to evaluate the significance of the model's difference from the perfect model (see supplemental Table S2 for thresholds used). An ideal LAI assimilated model will improve the R^2 from the non-LAI adjustment and will have a low z-score indicative of a small mean bias compared to the perfect model.

2.3.1 Model Configuration Sets

Besides the calibration soil and genetic coefficients, we designed a series of model simulations to isolate and combine effects of unknown soils and cultivars, proposing LAI assimilation could serve as a constraining factor to bring simulations with uncertain calibrations more in line with the default baseline model configuration's simulation. Cultivars and soils were swapped in without re-calibrating the full set of internal state variables.

To investigate the ability of LAI assimilation to constrain simulations with uncertain soil information, we utilized the five generic (uncalibrated) soil parameters as the starting point for the baseline simulations. Soil data was sourced from the SSURGO dataset for the field locations. Location-specific soil test data were not included for each plot. Differentiation of LAI assimilation performance based on specific soil parameters is beyond the scope of this study.

To synthesize conditions where the selection of a cultivar is uncertain, we created configurations for four cultivar alternatives to PC0004 which may be used in this region (Table 1). In addition to the calibrated cultivar, these included generic varieties characterized by their temperature response (LowGDD and HighGDD to maturity) and two previously calibrated cultivars that have historically been widely used in Iowa (Pioneer 3394, which is included in the standard DSSAT release, and an unreleased Pioneer 3394 parameter set). The LowGDD and HighGDD options only differed in the P1 parameter, which puts their growing-degree-day requirements at 2600-2650 and 2750-2800, respectively. The Pioneer 3394 options representing cultivars differing in more complex ways from the baseline cultivar.

Table 1. Cultivar parameters used in the experimental design.

Name	VRNAME	ECO#	P1	P2	P5	G2	G3	PHINT
Calibrated	PC0004	IB0001	240	0.75	850	800	8.5	49
LowGDD	PC0002	IB0001	185	0.75	850	800	8.5	49
HighGDD	PC0005	IB0001	260	0.75	850	800	8.5	49
Pio1	IB1067	IB0001	240	0.5	900	820	8.5	48
Pio2	ZZ0067	IB0001	246.5	0.611	761.2	818.8	8.28	75

VRNAME = Cultivar code; ECO# = Ecotype code; P1 = Thermal time from emergence to the end of juvenile phase (℃*days); P2 = Delay for each hour increase in photoperiod; P5 = Thermal time from silking to physiological maturity (℃*days); G2 = Maximum possible number of kernels per plant; G3 = Grain fill rate during linear grain fill stage and under optimal conditions (mg/day); PHINT = Phyllochron Interval: thermal time interval between successive appearances of the leaf tip (℃*days).

2.3.2 LAI Assimilation Strategies

LAI assimilation strategies were separated into 4 ensemble options: No LAI, Single-day, Window, and Continuous. For the No LAI ensemble, no remotely sensed adjustment was made to the simulated LAI in the crop model. The other ensembles describe different LAI assimilation schedules. In the Single-day ensemble, a remotely sensed LAI adjustment was made on one of six Julian days corresponding to phenological stages: flowering – Julian days 193 and 197, early grain filling – Julian days 213 and 217, and late grain filling – Julian days 257 and 261. For the Continuous ensemble, LAI adjustments were made to the crop model using all available dates between Julian days 160 and 270. For the Window ensemble, LAI adjustments were made to the crop model for all measurement dates available during a Julian day window: mid-vegetative (160-174), late-vegetative (175-189), flowering 190-204, early grain filling 205-219, mid grain filling 220-234, mid grain filling (235-249), and late grain filling (250-264).

We name each simulation according to patterns describing the soils and cultivars as well as the LAI assimilation schedule (Table 2). For soils and cultivars, ensemble number was combined with an abbreviated cultivar (e.g. generic, or uncalibrated, soil with HighGDD would be ‘’Gen_HighGDD’). For LAI assimilation, the “D”, “C”, and “W” represented single-day, continuous, and window updates, respectively. The associated Julian days for each strategy were combined with an underscore (e.g. single-day on Julian day 193 would be “D_193”). Continuous simulations used LAI information every 4 days and received the label “C_4”.

***Table 2**. Soils, cultivars, and LAI assimilation schedules used in combination within this study’s sensitivity tests, along with their abbreviations.*

a) Soils

Soil	Abbreviation
Calibrated	Cal
Uncalibrated (Generic)	Gen

b) Cultivars

Cultivar	Abbreviation
Calibration	Cal
Low GDD	LowGDD
High GDD	HighGDD
DSSAT Pio3394	Pio1
Unreleased Pio3394	Pio2

c) LAI Assimilation Schedule

Schedule	Abbreviation
None	No LAI
Single Day	D
Window	W
Continuous	C

3 Results

3.1 2002-2020 Simulations without LAI assimilation

Analysis indicates cultivar selection has a larger impact on model performance than the selection of soils as evidenced by the larger decline in R^2 when changing cultivars in Table 3. R^2 for the LAI integrated models with the baseline ranged from .790 to .994, meaning the models captured the variance to the perfect model well. The generally high R^2were expected given the soil and cultivar changes represent relatively minor modifications to the calibrated experiment setup given the management and weather were unchanged. All z-scores were significant at the $p<0.05$ level, with smallest absolute value of $z=1.96$ for the calibration cultivar with the generic soil. Raw z-scores are provided in supplemental Table S1. These high z-scores, resulting in low p-values for similarity, indicate the modified models struggled to capture the yield magnitude of the perfect model. Both metrics indicate room for model improvement using data assimilation to better reproduce the perfect model.

***Table 3**. Performance of simulation configurations without LAI assimilation. The R^2 of each cultivar and soil combination, compared to the default simulation (using calibrated cultivar and calibrated soils) perfect model yields for maize years between 2002 and 2020 based on NASS CDL land use datasets, indicates a reduction in captured variance that data assimilation would seek to overcome. P-values on mean bias are delineated by symbols (Table S2), with lower values indicating significant differences between the modified models and the perfect model (thus leaving space for data assimilation improvement).*

Cultivar	**Calibrated Soil**	**Generic Soil**
Calibration Cultivar	*[default configuration]*	0.994*
Generic LowGDD	0.913^	0.916#
Generic HighGDD	0.955^	0.951^
DSSAT Pioneer 3394 *(Pio1)*	0.973^	0.978^
Unreleased Pioneer 3394 *(Pio2)*	0.814^	0.790^

* denotes significance at p<0.05 level; # significant at p<0.01 level; ^ significant at p<0.001 level

R^2 and z-score differences across varieties were linked to distinct cultivar traits (recall Table 1). The HighGDD generic cultivar more closely tracked the calibration cultivar than the LowGDD cultivar (higher R^2), likely owing to having a more similar early season thermal time (P1; all other parameters were the same) to the calibrated cultivar. Pio1 had the greatest R^2 while Pio2 had the lowest. The Pio2 variety deviated from the current suite of cultivars through its lower grain filling rate (G3) and greater time between new leaf initiation (phyllochron interval; PHINT). Z-score magnitudes for Generic LowGDD and HighGDD were approximately similar, biased lower and higher, respectively, than the calibration cultivar. Mean bias was substantially greater for both Pio1 and Pio2 varieties.

Soil had a minor impact on R^2, as swapping the generic soil for the calibrated soil (columns in Table 1) had a small effect regardless of cultivar used ($\Delta R^2 \leq 0.24$). The generic soils had a slightly lower R^2 than the calibrated soil for the LowGDD and Pio1 cultivars, although these changes are tiny and may reflect fortuitous bias combinations. Generic soils push mean yields higher, which partially compensates for the LowGDD bias improving the z-score.

3.2 LAI assimilation in contrasting years

LAI adjustment inputs were successfully integrated into the CERES-Maize crop model by feeding MODIS LAI observations into the modified DSSAT Pest Module, as illustrated for a single test plot in 2016 within Figure 4. Looking first at the yellow line representing the baseline crop simulation without LAI assimilation, 2016 had relatively high yields in this region, with the baseline model showing simulated LAI peaking near 5 m^2 m^{-2} on Julian day 204 with gradual decay until Julian Day ~231 and then steeper decay until harvest.

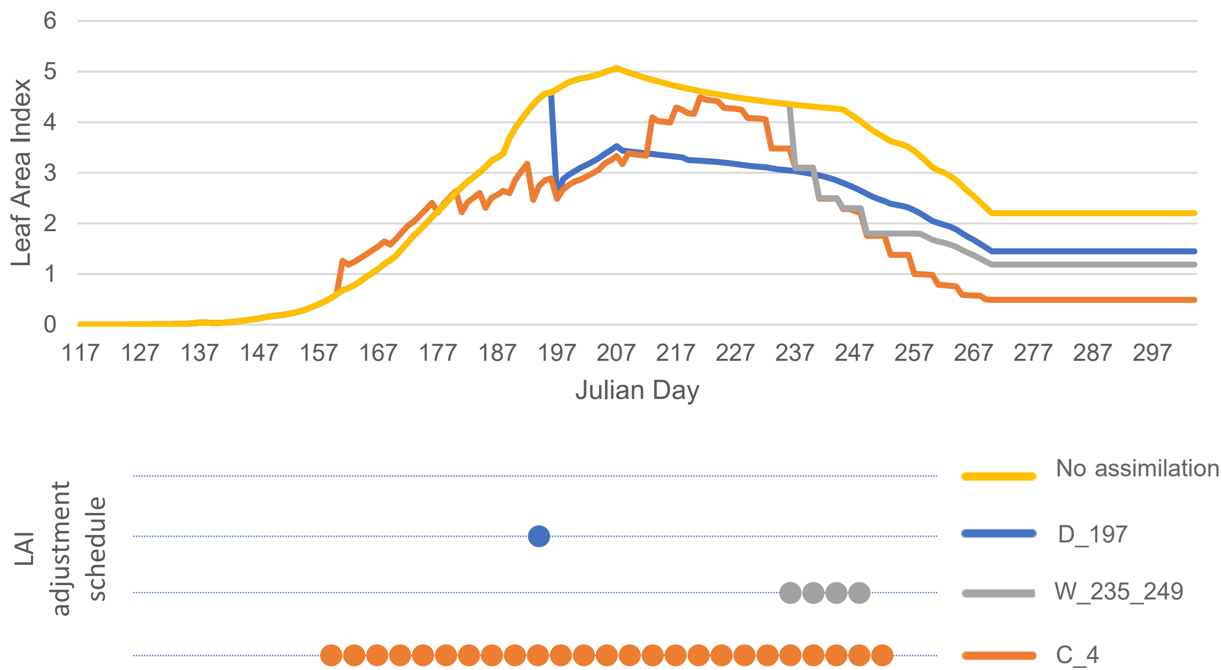

Figure 4. Impact of LAI Adjustments to CERES-Maize simulated LAI using the calibrated configuration (top), with schematic of corresponding LAI adjustment schedule for each assimilation strategy by day of year (bottom). D_197 = Single day update on Julian day 197; W_235_249 = Window update between Julian days 235-249; C_4 = Continuous 4-day updates.

The single-day LAI assimilation on day 197 (D_197; blue line) causes an immediate drop in LAI and results in an earlier peak of only ~4.5 m^2 m^{-2} and lower LAI through the remainder of the season. The model continued to increase LAI after the day 197 adjustment following the same pattern as the no-assimilation model given matching phenological progression but never achieving the baseline's maximum LAI before grain filling.

The window assimilation adjusts simulated LAI for four consecutive 4-day MODIS observations (W_235_249; gray line), resulting in a late-season drop in LAI earlier and steeper than the no assimilation baseline simulation. This adjustment was applied during grain filling, when leaf growth subsided and carbon was remobilized out of leaf tissue to support grain growth. In this case, leaf area continued to decrease because of carbon remobilization to seeds.

Finally, the continuous 4-day MODIS update simulation (C_4; orange line) appeared disjointed and inconsistent. The assimilation imposed an earlier and steeper green-up, a delay in the peak LAI by at least 10 days (although reaching a similar maximum of ~5 m^2 m^{-2}), and a more rapid decline during grain filling at the end of the season. Taken together, these example adjustment schedules show how LAI assimilation can impose different seasonal canopy structure on the crop simulation model, with even single-day and window interventions having effects capable of lingering throughout the remaining season.

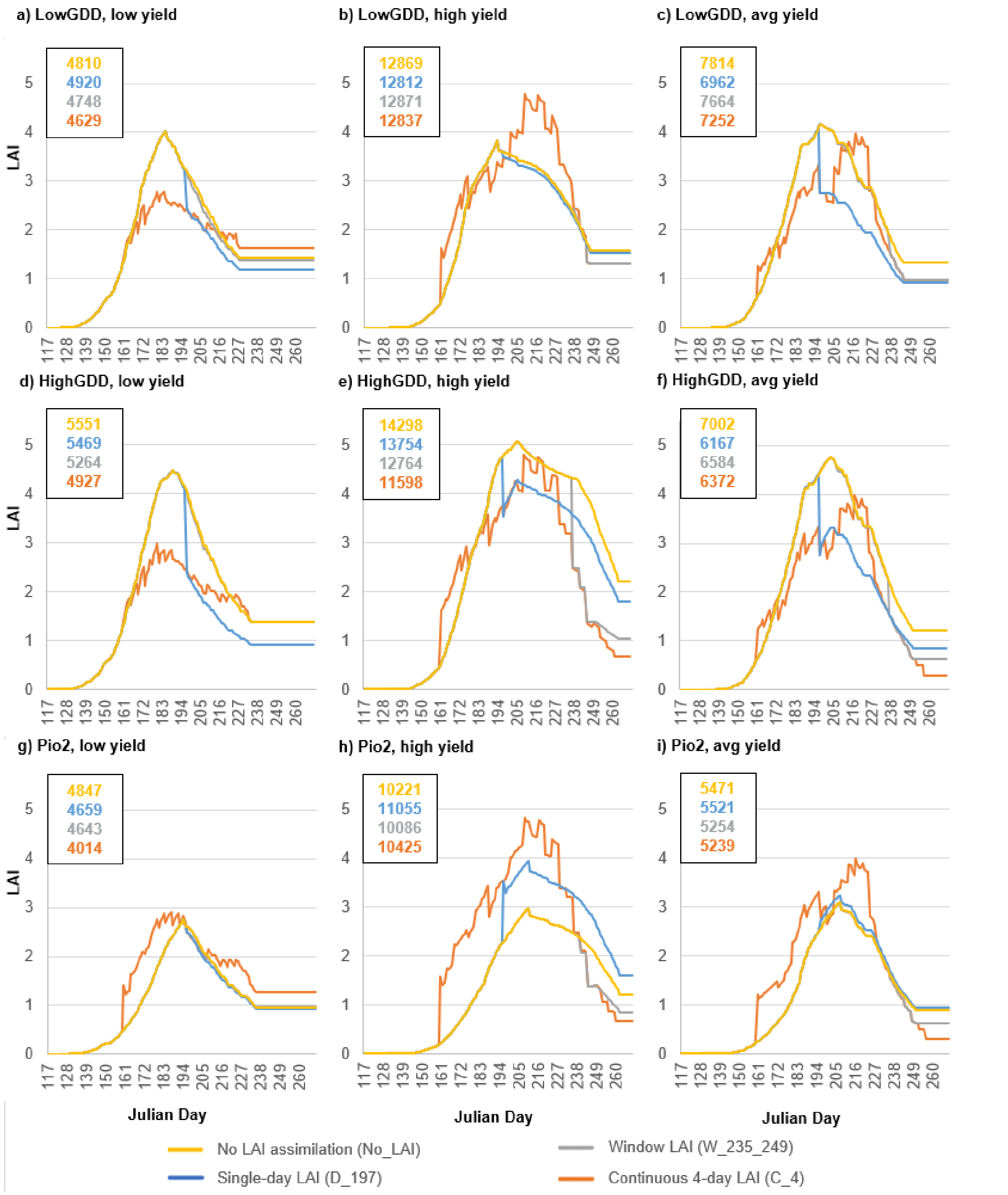

Figure 5. LAI responses to different satellite LAI assimilation schedules for different cultivars and example seasons. LowGDD (a-c), HighGDD (d-f), and Pio2 (g-i) for a low-yielding, dry year (2012, left column), a high-yielding, wet year (2016; middle column), and an average year (2020; right). Yields for each simulation are displayed in the upper-left corner of each panel with corresponding colors. Pio2 was included to represent a substantially different cultivar parameter set. Note,Perry was affected by the derecho (severe wind event) that swept across Iowa on August 10th, 2020 (Julian Day 224), leading to a decrease in LAI as seen in the C_4 line.

Figure 5 shows how corn in one of the Perry grids responds according to the interplay of different LAI adjustment strategies (No adjustment, single-day D_197, window W_235_249, and continuous C_4) and cultivars (LowGDD, HighGDD, and Pio2) across representative lower (2012), higher (2016), and relatively average (2020) yielding seasons (Schnitkey 2017, Paulson et al 2024). Because the experiment design used fixed days and windows for LAI assimilations, cultivar differences and weather-driven effects on seasonal phenological development can shift LAI constraints away from critical events, such as early season vegetive growth, peak LAI, and reproductive stages. Yield generally is higher for simulations and years when LAI is higher, although there is not any direct rule the highest average, peak, or end of season LAI guarantees the highest yield. This reflects the role of water, nitrogen, and heat stresses affecting the plant at key phenological stages as well as the potential for limiting biophysical processes not reflected in the LAI variable (e.g., reduced grain numbers). Further exploration of these stresses is beyond the scope of this study but represent a notable gap in understanding to be addressed in future work.

Drier and warmer conditions in 2012 led to a poor growing year for all cultivars (Fig 5a,d,g), with lower simulated and measured LAI along with a shorter season that interacted with the LAI assimilation schedule. Early season LAI measurements matched the LowGDD and HighGDD simulations well, while Pio2 substantially underestimated vegetative growth. Because 2012 was also a relatively warm year, peak LAI occurred between Julian day 184 and 195, prior to the single-day D_197 adjustment and over 2 weeks earlier than the peak LAI measured in 2016 for the calibration cultivar in the baseline scenario. All cultivars approximated the peak LAI timing well, however the baseline Pio2 approximated peak LAI magnitude while the other cultivars substantially overestimated. Crop maturity also occurred earlier, around Julian day 235. This led to the window W_235_249 LAI adjustment occurring during the grain filling stage rather than as a constraint on peak LAI. Pio2 baseline results again matched the LAI measurements well, specifically during the early reproductive stages, and underestimated LAI toward harvest. The LowGDD and HighGDD overestimated LAI during the early grain fill and underestimated LAI during late grain fill. All simulations agreed that the dry and warm year was the lowest yielding of the three years for each cultivar, with yield differences across assimilation strategies smaller than the year-by weather response.

Wet conditions in 2016 (Fig 5b,e,h) led to a better than average yield for all cultivars, with a higher peak LAI and longer season. Peak LAI was achieved between Julian day 195 and 215. Similar ranges in peak LAI and harvest timings were seen in the more typical precipitation year of 2020 (Fig 5c,f,i). Early season LAI measurements were greater than baseline simulations for all 2016 and 2020 plots, driving an upward LAI adjustment. For C_4 simulations, LAI measurements increased the peak LAI and typically shifted the LAI peak later in the season (Fig 5b and Fig 5i). Improved growing conditions extended the harvest to around day 260. The effects of cultivars, weather, and LAI adjustments accumulate to drive the largest differences between simulations in the reproductive stages (e.g., largest spread of lines in Fig 5.e; Fig 5.h) In some cases the timing of LAI assimilation fell on days where the model and observations were in close agreement, which led to a smaller adjustment and more consistent LAI development across simulations (e.g., 5.b, and Fig 5.i). This underscores the importance of aligning the LAI adjustments with desirable phonologic conditions and periods when models may drift further from observations. LAI assimilation did not overwhelm the larger yield impacts of year-by-year weather variability, with the wettest year always being the highest yielding.

The seasonal cycle of LAI is strongly influenced by the cultivar, which affects phenological development and peak LAI values. The single parameter (P1) that differentiates the LowGDD and HighGDD cultivars for this study (Table 1) constrains the thermal time between seedling emergence to the end of the juvenile phase. A larger P1 value requires a greater duration of time with temperatures greater than the Growing Degree Day threshold (8℃) before the flowering stages (tasseling and silking). LowGDD and HighGDD baseline and LAI assimilation strategies performed similarly until around Julian day 170 for all years, with HighGDD leading to the largest and latest peak LAI in all seasons as it had a longer vegetative stage. Pio2's phenology was similar to the HighGDD cultivar, but the overall LAI was reduced given the larger phyllochron interval (PHINT), which reflects longer thermal time necessary between successive leaf tip emergence (reducing the extent of green up). LAI assimilation acted to harmonize the seasonal cycle of LAI, with the continuous C_4 assimilation leading to nearly identical LAI patterns across cultivars within each season, although differences in C_4 yields show the effect of cultivar traits.

The performance of LAI assimilation is also responsive to cultivar differences which can further complicate the efficacy of LAI assimilation schedules. Using 2020 daily D_197 as a benchmark, LowGDD (Fig 5c) peak LAI was relatively aligned with the peak simulated LAI, leading to the simulation having the same peak LAI but lower values for the remainder of the season. In contrast, HighGDD (Fig 5f) simulated LAI would have continued to rise if not for the D_197 adjustment before flowering, affecting both peak LAI and the remainder of the season. For Pio2, simulated LAI deviated greatly from the measured LAI during the early season, indicated by the large increase in LAI for the C_4 assimilation scheme at 161, the first assimilation event. Pio2 peak LAI timing was similar to HighGDD with the D_197 adjustment minimized by the close values between observations and simulated values on that day. All three cultivars have lower simulated LAI than the observations in the early grain fill stages as cooler 2020 temperatures led to slower phenological growth and a later peak LAI.

3.3 2002-2020 Simulations with LAI Assimilation

An ideal assimilation would improve the model's R^2 and mean bias z-scores compared to the non-LAI model (top row) and not have a significantly different mean bias compared to the perfect model (top left corner). Table 4 shows the R^2 of the 9 maize growing seasons averaged across each of the 100 field locations for every LAI adjustment strategy. Highlighted cells indicate where the LAI adjusted model outperformed the respective no-LAI integrated simulation with the same soil and cultivar modifications (top row of the table, consistent with Table 3), indicating a benefit when LAI assimilation brought a simulation with alternative cultivars and/or soils more in line with the fully calibrated simulation. Definitionally, the upper-left $R^2 = 1.0$ because this is the calibrated configuration (calibrated soils and cultivar with no LAI) compared against itself. Underlined cells signify improvement in the z-scores for mean bias calculated against the perfect model (Table S1). Considering the non-assimilation values were all substantially different than the perfect model (Table 3), a reduction in z-scores (corresponding to an increase in p-values) indicates the modified model with assimilation is more in line with the perfect model's mean than the non-assimilation version of the modified model. Symbols in Table 4 show where p-values are not significantly different than the perfect model, indicating higher fidelity.

Table 4. *Analysis of modified model performance with and without LAI assimilation. The R^2 of simulated yields to the calibrated model for 9 years in the maize portion of the maize-soybean rotation (even years from 2004-2020), averaged across all 100 points at the test location. Rows are indicated by type of LAI adjustment strategy and the corresponding Julian day of the LAI adjustment date or period as well as an approximation of the corresponding expected maize development stage according to the baseline simulation. Gray shading shows R^2 exceeding the reference 'no LAI' simulation, and underlined values indicate z-score mean bias improvement compared to the reference 'no LAI' simulation. Unless otherwise indicated by symbols, all modified models remain significantly different from the perfect model at the p<0.001 level.*

		Calibrated Soils					Generic Soils				
Update schedule		Cal	LowGDD	HighGDD	Pio1	Pio2	Cal	LowGDD	HighGDD	Pio1	Pio2
No LAI updates	no LAI	1.000	0.913	0.955	0.973	0.814	0.994$^{\#}$	0.916^	0.951	0.978	0.790
Single-day LAI updates	D_193 Flowering	0.971	0.927	0.951*	0.932	0.833	0.972$^{\#}$	0.929	0.952$^{\#}$	0.940	0.804
	D_197 Flowering	0.967	0.928	0.942^	0.940^	0.830	0.970	0.932	0.946*	0.948	0.802
	D_213 Early Grain Fill	0.971	0.919	0.932	0.927*	0.793	0.981	0.923	0.951^	0.940	0.761
	D_217 Early Grain Fill	0.981	0.925	0.958	0.947	0.803	0.985^	0.927	0.965*	0.955	0.770
	D_257 Late Grain Fill	0.984^	0.914	0.941*	0.949	0.820	0.988*	0.918	0.946*	0.955	0.808
	D_261 Late Grain Fill	0.985^	0.917	0.935*	0.947	0.786	0.988*	0.920	0.938*	0.950	0.773
Window LAI Updates	W_160_174 Mid Veg	0.974*	0.913	0.941^	0.930	0.758	0.973*	0.920*	0.936	0.933	0.747
	W_175_189 Late Veg	0.984	0.922	0.962*	0.956	0.895	0.983^	0.929	0.959$^{\#}$	0.962	0.872
	W_190_204 Flowering	0.961	0.912	0.938	0.921*	0.847	0.960	0.916	0.938^	0.927^	0.821
	W_205_219 Early Grain Fill	0.946	0.921	0.934	0.910*	0.794	0.945	0.924^	0.941	0.917	0.763
	W_220_234 Mid Grain Fill	0.968	0.928	0.942	0.930$^{\#}$	0.788	0.967	0.929	0.951$^{\#}$	0.940	0.756
	W_235_249 Late Grain Fill	0.982	0.922	0.963	0.954*	0.791	0.985	0.924	0.962	0.958	0.761
	W_250_264 Late Grain fill	0.977	0.905	0.949	0.949	0.798	0.981^	0.909	0.944$^{\#}$	0.951	0.781
Continuous LAI Updates	C_4	0.979	0.909	0.931	0.946	0.781	0.982	0.912	0.931	0.948	0.773

* denotes p>0.05 level; $^{\#}$ denotes p>0.01; ^ denotes p>0.001

The extent to which LAI adjustment resulted in improved performance (compared to the no LAI simulations) varied according to LAI adjustment strategies and timing as well as the use of generic cultivars and soils. The first column represents the isolated effects of LAI adjustments when using the same cultivars and soils as the calibrated simulation. With no way to improve the perfect model, this column identifies LAI assimilation strategies leading to larger drops in R^2 and higher z-scores. Large deviations indicate the given LAI assimilation had a notable effect on the calibrated simulation (as described in Section 3.2). The lowest R^2 in this calibrated soils and cultivar column came from the early grain fill window adjustment W_205-219 (0.946), a period that often includes peak LAI where there can be large differences between simulated and observed LAI. The lowest R^2 amongst single-day adjustments in this column, D_197 (0.967), is similarly around peak LAI and the transition from flowering to early grain filling stages just before day 200. Notably, the continuous LAI updates C_4, using the calibrated cultivar, had a higher R^2

(0.979 in lower left cell of Table 4) than did any No-LAI simulation with an alternative cultivar (top row of Table 4), indicating that the observed LAI sequence was highly compatible with the calibrated simulations that serve as our basis for comparison.

LAI assimilation impacts on model bias (z-score) did not always track with the improvement or degradation of R^2. Cultivar and soil combinations not showing R^2 improvement often showed a mean bias improvement instead (as denoted by underlines in Table 4). In the case of the Pio1 cultivar with calibrated soils and LAI assimilation D_213, the assimilation removed mean bias to a level where it was indistinguishable from the perfect model but reduced R^2 compared to the no-LAI version. For Pio2 improvements in mean bias were still not enough to bring it close to the perfect model. In contrast, many of the LAI assimilations leading to improved R^2 increased the mean bias. The lone combination where R^2 improved and mean bias improved to the point where the modified model had a statistically indistinguishable mean bias from the perfect model was the generic soil HighGDD assimilation on day 217 (early grain fill).

LAI adjustments throughout the season can lead to improvements, although mean bias improvements were slightly reduced in the early and later growth stages. Early in the season LAI is low in both observations and models, so there is not much room for adjustment. Adjustment toward the end of the season may come after grain numbers are set and grain filling is well underway, perhaps reflecting that the adjustment was too late to differ substantially from the no-LAI approach. Mean bias improvement was most notable for HighGDD, generally reducing LAI during the season in a manner that reduced error injection.

In analyzing the effects of different LAI assimilation strategies across soils, we first note the generic soils (right half of the table) generally performed similarly to the calibrated soils (left half of the table) when evaluating R^2. This includes the overall pattern amongst particular combinations of LAI adjustments and cultivars that resulted in improved performance compared to the no LAI simulation. R^2 values for the same cultivar and LAI assimilation strategy (but with different soils) largely differed by less than 0.01, with the exceptions revealing that the Pio2 cultivar was most responsive to soil types. When using the calibrated cultivar, the generic soil had a very high R^2 with the calibrated soils version (R^2=0.994) which no LAI assimilation strategy could improve upon.

LAI adjustments had the largest positive effect on R^2 for the LowGDD cultivar in a manner that suggests a substantial ability to offset some of the bias for incorrect phenology. While the LowGDD parameter was improved with every daily assimilation update, most window updates, and the continuous update, the HighGDD cultivar was only improved for select daily and window assimilations. LowGDD and HighGDD are identical for all cultivar parameters but P1, which sets the thermal time for the vegetative stages associated with the green up period leading to peak LAI (recall Table 1) with effects on canopy lasting throughout the reproductive stages. For both generic cultivars LAI assimilation benefits were maximized by incorporating LAI observations just after peak LAI around the transition from early to mid-grain fill (Julian days 217 to 234). In this period (which is also the period with the largest R^2 improvement for Pio2) the crop model determines how much energy the plant can transfer from biomass to grain. This timing is beneficial for correcting cultivars with underestimated P1 (which have lower and earlier peak LAI) by increasing the given photosynthetic area with respect to biomass, while reducing biomass from cultivars with an overestimated P1 (which have later and higher peak LAI). Notable improvement was also seen in the earliest window, as this captures interannual variation in early season emergence and vegetative performance. LAI substantially improved the Pio2 cultivar mean bias and R^2, underscoring that LAI assimilation is most useful when constraining more erroneous configurations and discrepancies that manifest in LAI anomalies. Looking again at the top row of Table 4, Pio1 had the top performance amongst alternative cultivars under the no-LAI simulation, while Pio2 was the lowest correlating option (and thus had more room for correction). LAI assimilation was able to improve Pio1 mean bias but did not improve Pio1 R^2, as subtle changes in cultivars (compared to the calibration cultivar) could not be substantially improved by LAI assimilation using observations that also introduced their own inconsistencies with the reference calibration model. While the LowGDD and HighGDD cultivars only differed from the calibration cultivar in the P1 cultivar parameter (vegetative stage thermal times), Pio1 is distinctive in P2 (photoperiod sensitivity) and G2 (seed number), which are less well captured in LAI observations, and P5 (reproductive stage thermal time) that may come too late to make a substantial discrepancy correctable by LAI constraints. Pio2 is substantially different in nearly all cultivar parameters, although its positive response to the same LAI assimilation strategies that improved HighGDD indicates that its response is largely adjusting for P1 inconsistencies. While Pio2's higher PHINT lowers LAI across the whole season (recall Fig 5), this has a smaller direct sensitivity to the timing of LAI adjustments. Even with assimilation-driven improvements, Pio2 results are weakest on both mean bias and R^2.

Results indicate the timing of an LAI constraint is more important than the length of that assimilation period. Daily and window adjustments around the same phenology show generally similar results for R^2 and mean bias improvement as both directly affect a period that is small in comparison to the season length. Each effectively leaves the simulation with a modified LAI that carries forward as the simulation independently completes the season, and their effect will depend on the alignment of the assimilation day or window with the underlying phenology and observational biases. The most constrained Continuous C_4 simulation does not improve any of the imprecise soil and cultivar simulations compared to the no-LAI configuration, with a slight mean bias improvement in Pio1 the only exception even as the mean bias remains large. This indicates that the model can suffer when forced to follow an LAI pathway that is more divorced from the internal phenology and stresses experienced by the simulation. The continuous simulation also increases the chance of exposing the simulation to any errors in the remotely sensed LAI observations.

4 Discussion

We have demonstrated a new pathway for publicly available data from space-based remote sensing resources to act as a constraint for LAI and yield simulated by process-based crop models when precise cropping system details are not known. Utilizing an updating method for integrating LAI into DSSAT through its Pest module was successful at assimilating LAI into the CERES-Maize model at the well-calibrated Perry field site in the heart of the Corn Belt. The Pest Module entry point allowed external data to be injected into DSSAT without substantial modification to the underlying code or structure of the model.

The performance of the CERES-Maize model was indicative of a well-designed crop model representing decades of field experiments and biophysical understanding built into the process-based model by agricultural experts. Selection of a high-quality starting model reduces the space available to demonstrate remote sensing improvements; however, improvement indicates LAI assimilation can correct uncertain model configurations. Future work may need to further explore alternative models, broader configuration and parameter uncertainty, and estimated initializations which are often the best available in some regional systems where data assimilation has a larger potential for positive influence.

For most years and cultivars, the LAI from MODIS trended lower than the calibrated simulation of LAI. In later parts of the year this may be due to saturation of satellite-derived LAI after canopy closure. Methods to address this obstacle of remote sensing datasets may be available (e.g., using Enhanced Vegetation Index instead of NDVI to calculate LAI; Fang et al., 2011) but are not the focus of this paper. Assimilation techniques that more smoothly blend imposed LAI with the prior simulated LAI (rather than using a wholesale replacement) may result in a gentler and more cohesive continuing simulation state.

While LAI assimilation constrained biomass and yields and brought uncertain cultivars into closer alignment, it did not overwhelm fundamental differences in cultivars or seasonal weather impacts. Targeted LAI assimilation near key phenological stages, such as emergence and early grain fill, brought the generic configurations more in line with the well configured and calibrated simulations. Benefits were more pronounced with larger gaps in cultivar parameters, particularly related to early season phenology (P1) and total biomass as influenced by the rate of leaf tip appearance (PHINT). While improvement were greater, LAI assimilation was not consistently successful in compensating for a poor model configuration through increased R2 and reduced mean bias.

LAI constraints for the Perry, Iowa example worked better as a targeted nudge than as a wholesale replacement. Single-day and window adjustments were most effective when applied to early portions of the season to constrain simulations which formed a discrepancy with observations, pulling the value back towards reality while otherwise allowing the model to proceed freely with its own internal consistency. Continuous simulations, which adjusted LAI with each new observation, were not helpful on balance because additional adjustments offset the beneficial adjustments, effectively imposing a seasonal biomass cycle divorced from the internal balances, phenology, and water, temperature or nitrogen stresses of the underlying simulations. Noise in LAI observations likely had the largest effect on the continuously updated simulations C_4, although uncertain results likely also sporadically aligned with single-day and window assimilation dates.

The strong effects of adjustment timing (within the season) on overall assimilation benefit underscore the distinct characteristics and importance of key phenological stages that should be recognized in future assimilation design. Assimilations in the early vegetative stages (when the crop focuses on leaf and biomass accumulation to maximize photosynthesis) and early grain filling stage (when the crop prioritizes carbon and energy transfer to the kernels) performed better than adjustments late in the season after maximum grain number is set and the plant has already redirected resources toward grain filling. These beneficial adjustments align with the early phases of green-up and conditions just after peak LAI, allowing assimilation to ensure model conditions are appropriate for subsequent key reproductive growth stages. LAI assimilation would be further improved by more frequent satellite observations or aligning observational adjustments with key phenological stages and crop conditions rather than fixed Julian days. However, this type of targeted instrument design is not practical for satellite platforms observing many agricultural regions and heterogeneous systems. Differences in phenological timing across seasons, such as planting delays (potentially +/- several weeks due to cold spells or wet conditions) or warm or cold seasons (accelerating or decelerating crop maturity), result in fixed Julian date adjustments affecting simulations at a different phenological stage each year. We recommend further work to create a system for LAI adjustments with aligned phenological constraints, which would require simulation frameworks that could call for an LAI assimilation based on current crop status.

The LAI assimilation simulations shed interesting light on the ways the model responds to a rapid adjustment in the biomass state variables. Unlike the 'generic pest' we use to rectify discrepancies between the observations and model biomass, these adjustments do not reflect a real-world consumption of plant matter and therefore break the mass balance for nitrogen and water resources across soils and plant organs. When imposing LAI reductions, the DSSAT Pest module effectively consumes plant assimilated nitrogen as part of its changes to leaf weight and leaf nitrogen weight. However, when LAI increases the modified Pest Module generates additional 'phantom' nitrogen to meet the demand. Similarly, adjusting the LAI upwards implies more evapotranspiration occurred in the model, and this method does not adjust soil water content based on adjustments to LAI. This may disrupt nitrogen and water balances for a given field and could result in an overestimation of plant organ N and H_2O and underestimation of soil N and H_2O when LAI decreases, as well as the opposite biases when LAI increases. Hints of this appeared when LAI adjustments reduced biomass and reduced water stress in the dry 2012 year (Figure 5). Precise closures of the nitrogen and water budgets were secondary to goal of constraining LAI and yield, although we recommend further research to more fully address N balances and phenology discrepancies which can affect resource efficiency, later season crop conditions and response to weather hazards.

Although the assimilation only directly affected a limited number of variables, the perturbations reverberated through linked processes to affect most, if not all, state variables and nutrient pools. Increasing the number of assimilation perturbations may therefore destabilize the model or render its biophysical processes less consequential than the assimilation itself. Following each adjustment the model is left with the same phenology and thus tries to follow a consistent seasonal pattern of growth and decay, as seen by the adjusted and unadjusted LAI lines being nearly parallel following adjustments before converging with senescence toward the end of the season in Figure 5. Apparent differences and non-parallel behaviors reflect that soils and plant nitrogen pools have a stronger influence on water and nutrient stresses which are missing in LAI observations. This finding motivates future work to assimilate LAI and additional nitrogen and water observations to constrain soil moisture, nutrient pools and phenology in addition to biomass.

Although our focus was the yield variable in light of direct interest from commodity traders and farm operators, observations of alternative state variables may hold additional promise for improving yield simulations. Here we utilized LAI observations to constrain total biomass but noted a clear need for observations such as phenology, soil nitrogen, soil water and total water transpired. Reducing biases in those variables through observations or land surface model outputs would lead to substantial improvements in water, nitrogen, and heat stress, as well as assuring appropriate alignment between hazardous conditions and the plant development stage. Expansion of the key data assimilation capabilities of CERES-Maize's Pest Module would allow for integration of more remote sensing and ground data (e.g., drawn from farmer tractors and combines), ideally in a manner that allows balancing across multiple state variables. Digital twins that combine observations, crop models, and land surface models would also open doors for further decision support related to farm resilience, resource management, and the development of new crop hybrids.

The Perry, Iowa, experimental station proved to be a useful demonstration site for low-cost LAI assimilation into CERES-Maize; however, it is likely that other sites and contexts may provide stronger contrasts and additional insights into the data assimilation application. As one main appeal of process-based crop models is their ability to apply biophysical relationships to estimate conditions beyond a model's original calibration, applying the data assimilation approach for more years, systems and sites would likely identify conditions where observations are particularly beneficial (or less helpful). Analysis showed that the generic gridded soils used in this study did not strongly contrast from the calibrated soils, so further work is needed to determine whether LAI assimilation could have helped constrain more contrasting soil conditions. This study was also limited by the number of years at the Perry field experiment, which enabled model configuration and calibration but did not provide long-term yield data for ground truthing. Comparison on the scale of available validation data would further elucidate the benefits or drawbacks of data assimilation, although additional biases may be introduced through voluntary reporting or when aggregating at broad data scales (e.g., country reports).

5 Conclusions

LAI adjustments at the Perry, Iowa, maize location demonstrate a low-cost observational assimilation implementation with the potential to offset uncertain configuration parameters for broader applications. The positive or negative impact of LAI adjustment on DSSAT's ability to simulate yield anomalies was dependent on the number and timing of assimilation events. In the case of a true "perfect model" calibration, introducing observational constraints via data assimilation also introduces observational errors (e.g., from instrument biases or observational resolutions that mix land uses). Away from the experimental fields and well-calibrated models at the Perry site, yield modeling of Iowa corn would likely benefit from a minimal number of targeted assimilation events to constrain the early vegetative and early grain-filling stages.

Within-season assimilation of observations using remote sensing data is particularly appealing for wide domain, seasonal gridded crop model applications where precise cultivar, soils, and management information are not precisely known. While aerial and satellite imagery allow for tuning of crop model configurations around land use, the presence of irrigation and the extent of nitrogen applied, these adjustments largely constrain the mean yield pattern rather than seasonal yield variation. Many farmers and value chain partners, who are committed in their geography, care more about capturing and explaining seasonal anomalies (good and bad years) than in using models to describe spatial patterns that are well-captured by ground-based surveys. Fully quantifying all aspects of a region at a sufficient scale to be relevant is a challenging task requiring substantial computational and data resources, particularly as farmers update their management approaches, equipment, and seed cultivars each year. This suggests high potential for satellite-based, within-season updates that better reflect each season's changing crop processes and field conditions. We recommend coordinated development of gridded crop models using the latest observations to target deterministic state variables in a biophysically-balanced but otherwise minimally invasive data assimilation routine.

Acknowledgements

Authors appreciate technical discussions with DSSAT developers (Cheryl Porter and Gerrit Hoogenboom) at the University of Florida, collaborators at the NASA Goddard Space Flight Center (Pang-Wei Liu, Rajat Bindlish, Jessica Erlingis), AgMIP collaborators (Meijian Yang, Jose Guarin, Jonas Jägermeyr and Cynthia Rosenzweig), and participants at DSSAT Sprints. Sanketa Kadam at Columbia University provided technical assistance in the processing of satellite information. NASA POWER weather data production was supported through the NASA Earth Science Division. This work was supported by funding provided by the NASA Earth Science Division for the GISS Impacts Group.

References

Bandaru, V., Yaramasu, R., Jones, C., César Izaurralde, R., Reddy, A., Sedano, F., Daughtry, C. S. T., Becker-Reshef, I., & Justice, C. (2022). Geo-CropSim: A Geo-spatial crop simulation modeling framework for regional scale crop yield and water use assessment. ISPRS J. Photogramm. Remote Sens. , 183, 34–53. https://doi.org/10.1016/j.isprsjprs.2021.10.024

Basso, B., Cammarano, D., & Carfagna, E. (2013). Review of crop yield forecasting methods and early warning systems. In Proceedings of the first meeting of the scientific advisory committee of the global strategy to improve agricultural and rural statistics, FAO Headquarters, Rome, Italy (Vol. 241).

Batchelor, W.D., B. Basso and J.O. Paz. (2002). Examples of strategies to analyze spatial and temporal yield variability using crop models. Europ. J. Agronomy 18, 141-158.

Batchelor, W.D., J.W. Jones, K.J. Boote and H.O. Pinnschmidt (1993). Extending the use of crop models to study pest damage. Trans of the ASAE Vol 36(2): 551-558.

Durand, J.-L., Delusca, K., Boote, K., Lizaso, J., Manderscheid, R., Weigel, H. J., Ruane, A. C., Rosenzweig, C., Jones, J., Ahuja, L., Anapalli, S., Basso, B., Baron, C., Bertuzzi, P., Biernath, C., Deryng, D., Ewert, F., Gaiser, T., Gayler, S., … Zhao, Z. (2018). How accurately do maize crop models simulate the interactions of atmospheric CO2 concentration levels with limited water supply on water use and yield? Eur. J. Agron., 100, 67–75. https://doi.org/10.1016/j.eja.2017.01.002

Fang, H., Liang, S., & Hoogenboom, G. (2011). Integration of MODIS LAI and vegetation index products with the CSM–CERES–Maize model for corn yield estimation. Int. J. Remote Sens. 32(4), 1039-1065. https://doi.org/10.1080/01431160903505310

Hoogenboom, G., C.H. Porter, K.J. Boote, V. Shelia, P.W. Wilkens, U. Singh, J.W. White, S. Asseng, J.I. Lizaso, L.P. Moreno, W. Pavan, R. Ogoshi, L.A. Hunt, G.Y. Tsuji, and J.W. Jones. (2019). The DSSAT crop modeling ecosystem. In: p.173-216 [K.J. Boote, editor] Advances in Crop Modeling for a Sustainable Agriculture. Burleigh Dodds Science Publishing, Cambridge, United Kingdom.https://dx.doi.org/10.19103/AS.2019.0061.10.

Hoogenboom, G., C.H. Porter, V. Shelia, K.J. Boote, U. Singh, W. Pavan, F.A.A. Oliveira, L.P. Moreno-Cadena, T.B. Ferreira, J.W. White, J.I. Lizaso, D.N.L. Pequeno, B.A. Kimball, P.D. Alderman, K.R. Thorp, S.V. Cuadra, M.S. Vianna, F.J. Villalobos, W.D. Batchelor, S. Asseng, M.R. Jones, A. Hopf, H.B. Dias, A. Jintrawet, R. Jaikla, E. Memic, L.A. Hunt, and J.W. Jones. (2024). Decision Support System for Agrotechnology Transfer (DSSAT) Version 4.8.5 (www.DSSAT.net). DSSAT Foundation, Gainesville, Florida, USA.

Jones, J.W., G. Hoogenboom, C.H. Porter, K.J. Boote, W.D. Batchelor, L.A. Hunt, P.W. Wilkens, U. Singh, A.J. Gijsman, and J.T. Ritchie (2003). The DSSAT cropping system model. European Journal of Agronomy 18:235-265 (https://doi.org/10.1016/S1161-0301(02)00107-7).Ines, A.V.N., N. Das, J.W. Hansen, and E.G. Njoku, 2013: Assimilation of remotely sensed soil moisture and vegetation with a crop simulation model for maize yield prediction. Remote Sens. Environ. 138, 149–164. Doi: 10.1016/j.rse.2013.07.018.

Jin, X., Kumar, L., Li, Z., Feng, H., Xu, X., Yang, G., & Wang, J. (2018). A review of data assimilation of remote sensing and crop models. Eur. J. Agron. 92, 141–152. https://doi.org/10.1016/j.eja.2017.11.002.

Jones, J. W., Antle, J. M., Basso, B., Boote, K. J., Conant, R. T., Foster, I., Godfray, H. C. J., Herrero, M., Howitt, R. E., Janssen, S., Keating, B. A., Munoz-Carpena, R., Porter, C. H., Rosenzweig, C., & Wheeler, T. R. (2017). Brief history of agricultural systems modeling. Agricultural Systems, 155, 240–254. https://doi.org/10.1016/J.AGSY.2016.05.014Martre, P., Wallach, D., Asseng, S., Ewert, F., Jones, J. W., Rötter, R. P., Boote, K. J., Ruane, A. C., Thorburn, P. J., Cammarano, D., Hatfield, J. L., Rosenzweig, C., Aggarwal, P. K., Angulo, C., Basso, B., Bertuzzi, P., Biernath, C., Brisson, N., Challinor, A. J., … Wolf, J. (2015).

Multimodel ensembles of wheat growth: many models are better than one. Glob. Change Biol. 21(2), 911–925. https://doi.org/10.1111/gcb.12768.
[DATASET] Myneni, R., Knyazikhin, Y., Park, T. (2021). MODIS/Terra+Aqua Leaf Area Index/FPAR 4-Day L4 Global 500m SIN Grid V061 [Data set]. NASA EOSDIS Land Processes Distributed Active Archive Center. Accessed 2024-07-15 from https://doi.org/10.5067/MODIS/MCD15A3H.061.
Paulson, N., G. Schnitkey and C. Zulauf. "Variability in Trend Estimates for US Corn Yields." *farmdoc daily* (14):72, Department of Agricultural and Consumer Economics, University of Illinois at Urbana-Champaign, April 16, 2024. https://farmdocdaily.illinois.edu/2024/04/variability-in-trend-estimates-for-us-corn-yields.html
Purcell, W., & Neubauer, T. (2023). Digital Twins in Agriculture: A State-of-the-art review. Smart Agric. Technol. 3, 100094. https://doi.org/10.1016/J.ATECH.2022.100094.
Pylianidis, C., Osinga, S., & Athanasiadis, I. N. (2021). Introducing digital twins to agriculture. Comput. Electron. Agric.184, 105942. https://doi.org/10.1016/J.COMPAG.2020.105942.
[DATASET] Ranga Myneni, Knyazikhin, Yuri, Taejin Park - Boston University and MODAPS SIPS - NASA. (2015). MOD15A3H MODIS/Combined Terra+Aqua Leaf Area Index/FPAR Daily L4 Global 500m SIN Grid. NASA LP DAAC. http://doi.org/10.5067/MODIS/MOD15A3H.006
Richetti, J., Boote, K. J., Hoogenboom, G., Judge, J., Johann, J. A., & Uribe-Opazo, M. A. (2019). Remotely sensed vegetation index and LAI for parameter determination of the CSM-CROPGRO-Soybean model when in situ data are not available. Int. J. Appl. Earth Obs. Geoinf. 79, 110-115. https://doi.org/10.1016/j.jag.2019.03.007
Rosenzweig, C., Jones, J. W., Hatfield, J. L., Ruane, A. C., Boote, K. J., Thorburn, P., Antle, J. M., Nelson, G. C., Porter, C., Janssen, S., Asseng, S., Basso, B., Ewert, F., Wallach, D., Baigorria, G., & Winter, J. M. (2013). The Agricultural Model Intercomparison and Improvement Project (AgMIP): Protocols and pilot studies. Agric. For. Meteorol. 170, 166–182. https://doi.org/10.1016/J.AGRFORMET.2012.09.011.
Rosenzweig, C., S.S. McDermid, E. Mencos-Contreras, S. Asseng, A.A. Chattha, T. Li, M. Madajewicz, S. Nedumaran, T.T.N. Nguyễn, A.C. Ruane, N. Subash, R. Valdivia, and G. Vellingiri, (2023). Integrated climate change assessments on selected farming systems in India, Pakistan, Bangladesh, and Viet Nam. In Fostering Resilient Global Supply Chains Amid Risk and Uncertainty. D. Azhgaliyeva, J. Beirne, D.B. Rahut, and Y. Yao, Eds., ADBI Series on Asian and Pacific Sustainable Development, Asian Development Bank Institute, pp. 67-95.
Ruane, A. C., Rosenzweig, C., Asseng, S., Boote, K. J., Elliott, J., Ewert, F., Jones, J. W., Martre, P., McDermid, S. P., Müller, C., Snyder, A., & Thorburn, P. J. (2017). An AgMIP framework for improved agricultural representation in integrated assessment models. Environ. Res. Lett. 12(12), 125003. https://doi.org/10.1088/1748-9326/aa8da6.
Schnitkey, G. “Variability in County Corn Yields: 2012 to 2016." farmdoc daily (7):139, Department of Agricultural and Consumer Economics, University of Illinois at Urbana-Champaign, August 1, 2017. http://farmdocdaily.illinois.edu/2017/08/variability-in-county-corn-yields-2012-to-2016.html
Sweet, L.-B., I.N. Athanasiadis, R. van Bree, A. Castellano, P. Martre, D. Paudel, A.C. Ruane, and J. Zscheischler (2025): Transdisciplinary coordination is essential for advancing agricultural modeling with machine learning. *One Earth*, **8**, no. 4, 101233, doi:10.1016/j.oneear.2025.101233.
Thorp, K. R., David Batchelor, W., Paz, J. O., Kaleita, A. L., & Dejonge, K. C. (2007). Using Cross-Validation to Evaluate CERES-Maize Yield Simulations within a Decision Support System for Precision Agriculture. Trans. of the ASABE. 50(4). http://lib.dr.iastate.edu/abe_eng_pubs.

Thorp, K.R., W.D. Batchelor, J.O. Paz, B.L. Steward and P.C. Caragea (2006). Methodology to link production and environmental risks of precision nitrogen management strategies in corn. Agric. Syst. 89 (2006) 272-298.

Thorp, K. R., Batchelor, W. D., & Paz, J. O. (2005). A cross validation approach to evaluate CERES-Maize simulations of corn yield spatial variability. In 2005 ASAE Annual Meeting (p. 1). American Society of Agricultural and Biological Engineers.

Thorp, K.R. and K. F. Bronson (2013). A model-independent open-source geospatial tool for managing point-based environmental model simulations at multiple spatial locations. Environ. Model. Softw. 50, 25-36.

White, J.W., G. Hoogenboom, P.W. Stackhouse, and J.M. Hoell (2008). Evaluation of NASA satellite- and assimilation model-derived long-term daily temperature data over the continental US. Agricultural and Forest Meteorology 148(10), 1574-1584, doi:10.1016/j.agrformet.2008.05.017.